



OPEN

DATA DESCRIPTOR

CORE-VTRCC Cruise Report: Geophysical Acquisition and Seafloor Sampling along the Vitória-Trindade Ridge

Gabriel Tagliaro¹✉, Mateus A. C. Gama², Adolfo N. Britzke², Vinicius H. A. Louro², Pedro Bauli², Gabriela C. Patines¹, Gabrielle D. Bonifatto¹, Ana C. B. Vieira¹, Beatriz B. S. Silva¹, Geandré C. Boni³, Luan K. Pantoja⁴, Paula P. Sergipe¹, Raylla S. Silva¹, Sarah A. Dos Santos⁴, Tainá N. Caram⁵, Tayná L. F. Pereira¹ & Luigi Jovane¹

This work reports the data obtained by the multidisciplinary cruise CORE-VTRCC surveying on the region around the Vitória-Trindade Ridge (VTR) aboard the vessel NHo Cruzeiro do Sul (October 18th to November 6th, 2021). The main objectives of the VTRCC Cruise were (1) to assess the role of the VTR as an oceanographic barrier for bottom currents along the Brazilian margin; and (2) to characterize the morphology of the volcanic seamounts and its relationships with the carbonate sediments that cover it. For that, we performed multibeam bathymetry, magnetometry, high-resolution multichannel seismic survey, subbottom profiling survey, and seafloor sampling along the VTR and along the Columbia Deepwater Channel. The raw dataset was processed for quality control and organized for public access. When required, additional geophysical processing occurred to improve data quality. Seafloor samples are characterized based on the concentration of its biofacies, the sediment grain-sizes and the morphology of rhodoliths sampled. The dataset reveals comprehensively the geological and oceanographic heterogeneity of the region around the VTR.

Background & Summary

In the southeast Brazilian Margin at latitude 20°S is located the Vitória-Trindade Ridge (VTR), a group of volcanic islands and carbonate banks that splits the deep Brazilian margin (>1000 m) in two oceanographic domains, north and south of the VTR¹. Formed by submarine volcanism since the Oligocene, the VTR seamount chain extends 1200 km offshore the Brazilian coast and is composed by numerous volcanic seamounts and carbonate banks^{2–5} (Fig. 1). The seamounts of the VTR rise up to 5 km from the oceanic crust seafloor, with multiple of the seamount's seafloor reaching the photic zone (Besnard, Jaseur, Columbia and Davis Bank). Consequently, the VTR represents an important barrier for ocean currents flowing along the Brazilian margin, which resulted in a complex and heterogenous environment regarding its physical, geological and biological constituency and evolution^{6–8}. Although rich and complex, little is still known about the seafloor and subsurface morphology of the region around the VTR.

The depositional systems around the VTR are marked by the interaction between ocean currents, volcanic seamounts and carbonate factories^{9–11}. In the deep (>3000 m), the steep volcanic slopes block the northward passage of the Antarctic Bottom Water Current (AABW) along the margin, while gravitational flows slip down the ridge to form a mixed contourite-turbidite depositional system^{11,12}. Such conditions may have influenced the formation of the turbidite-contourite Columbia Channel (CC) at the southern region of the VTR, along the displacement of the AABW^{11–13}. At water depths between 1000–3000 m, the southward flowing North Atlantic Deep Water (NADW) passes through the bathymetric gaps along the VTR (Fig. 1)¹³. Within the photic zone

¹Instituto Oceanográfico, University of São Paulo, São Paulo, Brazil. ²Instituto de Geociências, University of São Paulo, São Paulo, Brazil. ³Department of Oceanography and Ecology, Federal University of Espírito Santo, Vitória, Brazil. ⁴Department of Geology, Federal University of Rio Grande do Norte, Natal, Brazil. ⁵Institute of Geosciences, Federal University Fluminense, Niterói, Brazil. ✉e-mail: gabrieltagliaro@usp.br

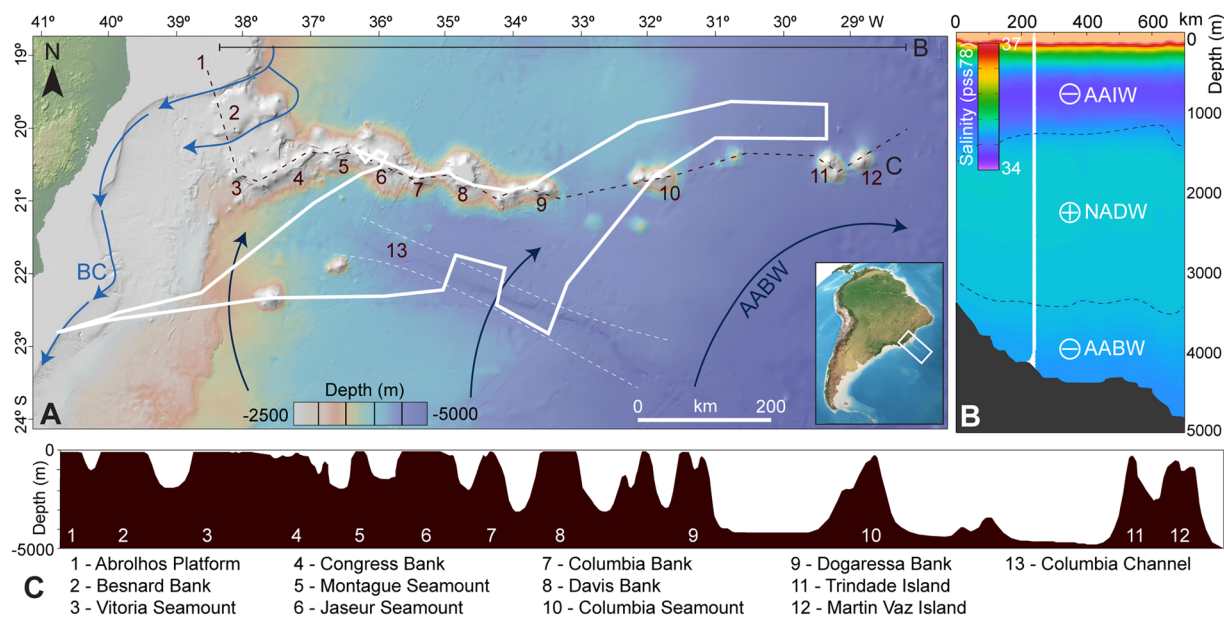


Fig. 1 (a) Study area and the track (white line) of the CORE-VTRCC Cruise across the Vitoria-Trindade Ridge (VTR) and the Columbia Channel (white dashed line)²⁶. (b) Current configuration in the region includes the south-flowing surficial Brazilian Current (BC), the north-flowing Antarctic Intermediate Water (AAIW) above 1000 m, the south-flowing North Atlantic Deep Water (NADW) between 1000–3500 m and the Antarctic Bottom Water (AABW) below 3500 m¹³. (c) Topographic profile along the VTR show the presence of numerous seamounts and carbonate banks/platforms. Nomenclatures are from the Brazilian Navy⁴⁰ and bathymetry from GRMT⁴¹.

(<100 m), reef communities thrived atop the volcanic seamounts, which formed carbonate platforms observed in the bathymetry as top planar surfaces^{10,14,15}. Red algae are the main constituents of the benthic fauna atop the VTR, but a rich and heterogenous habitat developed^{14,15}. The action of waves and surface currents over the carbonate factories triggered the formation of rhodolites, carbonate nodules formed by coralline red algae that move across the platform' surface under the action waves and currents¹⁴. Rhodolites thrive within the VTR, under the influence of the Brazilian Current^{14,15}.

In order to better characterize the marine environment around the VTR, the Cruise CORE-VTRCC was organized in late 2021 by the Oceanographic Institute of the University of São Paulo in partnership with the Brazilian Navy (Directorate of Hydrography and Navigation – DHN), to acquire geophysical data (seismic data, bathymetry, magnetometry) and seafloor samples in the region along the VTR, including the continental slope, the volcanic seamounts, the carbonate factories atop the seamounts, and the deepwater channels of the region. The research vessel NHo Cruzeiro do Sul was assigned for that cruise due to its geophysical and sediment sampling capabilities. The cruise departed the city port of Niterói on October 18th of 2021 and returned on November 6th of 2021, to a total of 18 days of cruise activities. The scientific group was composed by 13 students and researchers from multiple Brazilian universities. In total, the cruise completed 1873.70 nautical miles, surveying 1513.50 nautical miles with multibeam bathymetry and sub-bottom profiler, 14 multichannel seismic lines, 31 XBT (Expendable Bathythermograph) profiles, and 9 sediment samples (Fig. 2). Seafloor depth across the survey area ranged from ~80 m atop the seamounts down to 5200 m near Trindade Island. Survey boundaries were 23° S, 19.65° N, 29.20° E and 40.81° W.

Methods

High-resolution multichannel seismic. Multichannel seismic data was acquired using a sparker seismic source with 800 tips model Geo-Source 800, up to 7 kJ energy power supply (GeoSpark 2000X) and a 48-channel streamer, all from the Geo Marine Survey Systems. Seismic acquisition and SEG-Y conversion were performed with the software GeoRecorder, also from Geo Marine Survey Systems. The Geo-Source 800 uses a negative discharge for seismic pulse generation which results in a more stable seismic signature with a frequency range between 200–3000 Hz, centered at ~1 kHz. The streamer is composed of three hydrophones per channel, with a total active length of 150 m and 2 × 25 m cable stretches, to a total of 200 m of streamer deployment. Channel distance in the streamer is 3.125 m and channel sampling occurred at 10 kHz. Geographic geometry was supplied by a DGPS antenna placed atop the seismic source configured with the WGS-84 ellipsoid and UTM projection zone 25S. Geometry distance averaged 5 m between source and streamer (dx) and ~20 m between source and first channel (dy; Table 1). The source was placed at 1.5 m water depth while the streamer was at 0.5 m water depth. Energy levels and trigger interval for pulse generation varied across the survey depending on the bathymetric profile (Table 1). Vessel velocity during seismic acquisition averaged 4 knots (Table 1).

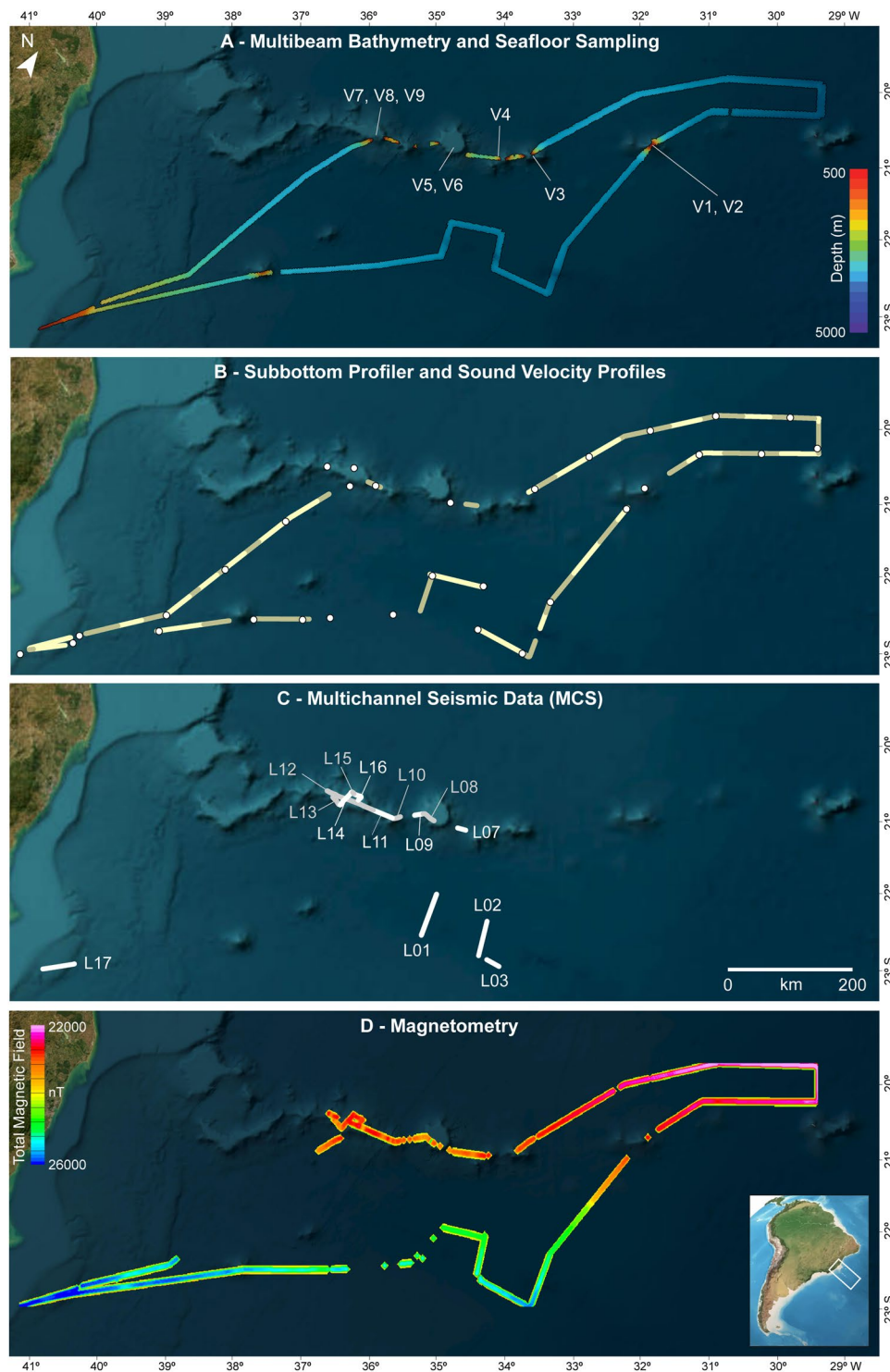


Fig. 2 Data acquired during the CORE-VTRCC Cruise. (a) Multibeam bathymetry survey occurred throughout the vessel track with the exception of shallow depths (<100 m). Seafloor samples were acquired atop the Columbia Seamount (V01 and V02), atop the Dogaressa Bank (V03 and V04), atop the Davis Bank (V05 and V06) and atop the Jaseur Seamount. (b) Sub-bottom and sound velocity profiles were also acquired throughout the cruise track but not at <100 m depths. (c) Multichannel Sparker Seismic data was acquired along the Columbia Channel (L01-L03), along the VTR (L07-L15) and at the Rio de Janeiro continental slope (L17). (d) Marine magnetometry was acquired throughout the survey track when sea conditions were safe.

Seismic Line	Vessel Velocity (knots)	Record Length (ms)	Trigger Length (ms)	Source Energy (J)	CMP gather (m)	Distance source and streamer – dx (m)	Distance source and streamer – dy (m)
MCS-L01	4.8	5000	5000	7000	6.25	5	13
MCS-L02_1	4.5	5000	5000	7000	6.25	5	15
MCS-L02_2	4.5	5000	5000	7000	6.25	5	15
MCS-L03	4.3	5000	5000	7000	6.25	5	25
MCS-L07	4.2	7000	7000	7000	6.25	5	25
MCS-L08_1	4.3	6000	6000	6300	6.25	5	25
MCS-L08_2	4.3	4000	4500	6300	6.25	5	25
MCS-L08_3	4.3	4000	4500	6300	6.25	5	25
MCS-L08_4	4.3	4000	4500	6300	6.25	5	25
MCS-L08_5	4.3	4000	4500	6300	6.25	5	25
MCS-L09	4.3	4000	4500	6300	1.562	5	30
MCS-L10	3.5	6000	6500	6300	1.562	5	30
MCS-L11_1	3.5	4000	4500	6300	6.25	5	13
MCS-L11_2	3.5	4000	4500	6300	6.25	0	35
MCS-L12	4	4000	4500	6300	6.25	0	21
MCS-L13	4	4000	4500	6300	6.25	5	25
MCS-L14	4.2	4000	4500	6300	6.25	5	25
MCS-L15	4.2	4000	4500	4950	6.25	5	25
MCS-L16_1	4.2	4000	4500	7000	6.25	5	30
MCS-L16_2	4.2	4000	4500	7000	6.25	5	30
MCS-L17	4	4000	4500	7000	6.25	5	30

Table 1. Main parameters used during the acquisition and processing of multichannel seismic data.

Seismic processing was performed with the software RadExPro v2022.1. Basic brutestack seismic processing was made for all seismic lines, following the steps: quality control (data filtering), preprocessing (noise filtering), geometry evaluation, normal moveout correction and stacking. For Lines L01 and L17 was performed an improved seismic processing, including the following additional processing steps: static correction, deconvolution, multiple suppression and migration. Bandpass filtering was performed between 200–1500 Hz. For stacking, common mid points (CMD) gathers were established according to Table 1.

Sub-bottom profiler. High resolution sub-bottom profiler data were acquired employing an SBP-120 from Kongsberg installed in the hull of the ship. Survey geometry came from a SeaPath 330 positioning system with two GNSS antennas without differential positioning. Acquisition occurred in the Kongsberg SIS software with the ellipsoid WGS-84 and a UTM projection with zone 25S. The equipment was operated with one main channel, in a frequency of 2.5–6.5 kHz, with chirp up linear pulse, which results in a maximum vertical resolution ~0.3 ms. The data was logged in Topas raw format and converted to SEG-Y format. The power of the SBP pulse and trigger interval varied along the survey depending on ocean conditions and seafloor depth. Survey velocities ranged from 4–7 knots.

Multibeam bathymetry and sound velocity profiling. Multibeam bathymetry was performed with the deep echosounder Kongsberg EM-122 with 12 kHz of operating frequency. The system was coupled with the SeaPath 330 positioning system with two GNSS antennas. Acquisition occurred in the Kongsberg SIS software with the ellipsoid WGS-84 and UTM projection. The swath width was set to automatic up to 55° with a ping frequency of 40 Hz. Due to the deep characteristics of the EM-122 equipment, multibeam bathymetry was not performed in water depths shallower than 200 m (Fig. 2). Survey velocities ranged between 4–7 knots.

To estimate sound velocity profiles for bathymetric processing, temperature profiles were first obtained for the water column throughout the survey every 50 nautical miles, to a total of 31 profiles. For that we used Expendable Bathythermograph (XBT) Lockheed Martin model T5 to the deeper portion of the survey (down to 1860 m water depth) and the model T7 over the shallower regions (down to 760 m). A salinity profile is then calculated by linearly interpolating the measured temperature profile to the nearest WOA/RTOFS salinity profile. Sound speed values are then calculated from the salinity updated profile using the UNESCO equation¹⁶. Vertical extrapolation of sound velocity profiles below 1800 m was performed with the UNESCO equation within the SVP editor using WOA09 CTD profiles down to 5500 m and Challenger Deep CTD profiles down to 12000 m depth^{17–19}. Sound velocities were then incorporated during the multibeam bathymetry acquisition directly into the SIS software.

Multibeam bathymetry preprocessing was performed on the software CARIS HIPS from Teledyne during the expedition. A Patch Test calibration of the echosounder was done atop the Columbia Seamount on October 26th, where roll, pitch, yaw, heading and the time delay were calibrated. The corrected values from the Patch Test were then inserted into the processing procedure. Finally, spike removal and surface equalization processing were performed with the software EIVA NaviModel Producer after the expedition.

Sediment Sample	Location	Seafloor Depth (m)	Longitude (DD)	Latitude (DD)
V1	Columbia Seamount	69	−31.834750	−20.731167
V2	Columbia Seamount	220	−31.801017	−20.701833
V3	Dogaressa Bank	80	−33.597407	−20.892483
V4	Dogaressa Bank	114	−33.988767	−20.917833
V5	Davis Bank	84	−34.702267	−20.809850
V6	Davis Bank	94	−34.693833	−20.811733
V7	Jaseur Seamount	57.8	−35.877833	−20.532133
V8	Jaseur Seamount	110.4	−35.899733	−20.593466
V9	Jaseur Seamount	99.1	−35.915367	−20.592700

Table 2. Sediment Sampling Sites. Geographic Coordinates were represented in Decimal Degrees (DD). The column Location corresponds to the name of Seamounts (Smt.) and Banks (Bk.) where the samples were collected.

Marine magnetometry. The SeaSPY magnetometer from Marine Magnetics was used to acquire the magnetic field data. The sensor (torpedo) was towed 250 m behind the vessel and 300 m from the vessel's GPS. Survey velocities ranged between 4–7 knots. The SeaSPY magnetometer is a Proton Precession (Overhauser) sensor of absolute accuracy, and the resolution of the system is 0.1 nT and 0.001 nT, respectively. The data was acquired in a 10 Hz frequency, from the continental slope to the furthest point from the continent, near Trindade Island. The frequency resulted in measurements for every meter traveled, on average, with the sensor about 30 to 35 m below the sea level. The survey also occurred in parallel to the seismic survey, without any perceptible interference.

In the processing step, the data had low-quality/high-noise measurements removed and was filtered using a non-linear filter of 10 fiducials to eliminate spikes from the data. The quality approved field was reduced using the International Geomagnetic Reference Field (IGRF) to correct long-wavelength effects non-related to crustal features. The resulting Total Magnetic Field was finally filtered using a first-order polynomial filter to highlight medium- to short-wavelength anomalies related to the VTR, producing the Residual Magnetic Field surveyed by the cruise.

Seafloor sediment sampling. During the expedition nine seafloor sediment samples were collected within the Vitória-Trindade Ridge with a Van-Veen grab sampler (3600 cm²) on the top of the volcanic seamounts (Fig. 2; Table 2). Sample V7 collected only rhodoliths, without additional sediments. Grain sizes larger than 40 mm diameter (pebble size) were separated for rhodolith measurements. Sediment samples were washed and dried to remove salt grains and other impurities. Sediment samples were bathed in a water container for 48 h, and the water medium was removed with a syringe. Finally, the decanted sediments were then oven-dried at 45 °C for 72 hours. For rhodolith samples, we dried samples at 35 °C for 48 hours. The morphometry of the rhodoliths was classified in spheroidal, discoidal and ellipsoidal based on the measurement of the long (L), intermediate (I) and short (S) axis with a Vernier Caliper (Tables 3, 4)²⁰.

Subsequently, samples had their weight measured and carried out the sieving in 13 phi fractions (−1.5, −1.0, −0.5, 0, 0.5, 1.0, 1.5, 2.0, 2.5, 3.0, 3.5, 4.0 and >4.0) for 10 minutes. Samples sieved were described in phi fractions, then were grouped in the following orders, according to Wentworth classification²¹: granules (−2 to −1 phi), very coarse sand (−1 to 0 phi), coarse sand (0 to 1 phi), medium sand (1 to 2 phi), fine sand (2 to 3 phi), very fine sand (3 to 4 phi) and silt (>4 phi). Mean grain sizes and sorting were analyzed on Gradistat v9.1 software²², using the parameters described by Folk^{23,24}. Sediment samples were also placed on a Petri dish for microscope analysis and photography using the Fiji software²⁵. Microscopic photographs were taken with a Zeiss Stemi DV4 stereomicroscope, at zoom scale of 8x and a total diameter of 26 mm. Grains were then classified in carbonate debris, foraminifers, bryozoans, sponge's spicules, bivalves, gastropods, crustaceans, echinoderms, and annelida, and its abundance was quantified based on 300 random point counts per sample.

Data Records

The final data and its descriptions are available at the Marine Geoscience Data System repository under the Creative Commons 4.0 International Public License (CC-BY 4.0). Navigation data is provided as an ASCII file at <https://doi.org/10.26022/IEDA/331475> with data, hour and UTM and geographic coordinates²⁶. Raw and high-resolution multi-channel seismic reflection are available in SEG-Y format (<https://doi.org/10.26022/IEDA/331494> and <https://doi.org/10.26022/IEDA/331485>)^{27,28}. Name structure follows expedition name VTRCC, method (MCS – Multichannel Seismic), line number, processing step (original data – RAW; stack – STK; and post stack time migration – PostSTM). Subbottom profiler data is available in SEG files (<https://doi.org/10.26022/IEDA/331484>)²⁹. Name structure follows VTRCC, method (Subbottom Profiler – SBP) and line number.

Raw multibeam swath bathymetry data is available in format Kongsberg.all (<https://doi.org/10.26022/IEDA/331477>)³⁰ while processed multibeam swath bathymetry is available in MB-System-compatible GSF format (<https://doi.org/10.26022/IEDA/331478>)³¹. Name structure follows line number, date and hour, and research vessel. Bathymetry grids are also available in format ESRI ASCII (<https://doi.org/10.26022/IEDA/331479>)³². XBT-derived Sound velocity profiles are available bundled in format.svp (<https://doi.org/10.26022/IEDA/331480>)³³. Data for each profile includes date and time, position, depth and sound velocities (m/s). Magnetometry data is available as an ASCII file at <https://doi.org/10.26022/IEDA/331476> with the headers geographic and UTM coordinates, magnetic field, residual magnetic field, date and time³⁴.

Sediment Sample	Rhodolith Specimen	Large Axis (mm)	Intermediary Axis (mm)	Short Axis (mm)
V1	1	48.26	45.37	32.72
V1	2	55.7	49.66	37.93
V1	3	104.56	73.35	72.08
V1	4	84.5	67.78	60.78
V1	5	85.49	69.28	58.67
V1	6	43.76	35.58	27.98
V1	7	49.66	36.9	27.23
V1	8	68.84	49.7	48.68
V1	9	76.5	69.22	63.58
V1	10	80.61	68.52	68.12
V1	11	122.78	68.12	54.04
V1	12	73.94	50.98	45.46
V1	13	95.72	76.62	73.03
V1	14	100.66	61.72	52.4
V3	1	149.16	90.11	87.28
V4	2	182.82	128.27	46.57
V4	3	86.17	74.42	71.21
V4	4	122.82	97.42	88.81
V4	1	142.96	102.58	65.44
V4	1	51.69	40.37	31.23
V4	2	35.45	30.43	21.79
V4	3	44.91	27.76	17.33
V4	4	22.73	22.25	21.07
V4	5	30.92	13.01	21.04
V4	6	32.52	25.03	13.64
V4	7	25.67	15.56	10.06
V6	8	20.39	16.26	13.88
V6	9	18.93	12.99	11.53
V6	10	21	17.04	10.59
V7	11	27.22	10.08	15.3
V7	1	84.52	31.05	11.81
V7	2	46.17	30.49	14.69
V7	3	23.11	20.37	13.37

Table 3. Morphometric measurements for Rhodolith samples V1-V7.

For the seafloor sediment samples, both macro and microscopic photographs are available in JPEG format at <https://doi.org/10.26022/IEDA/331483>³⁵. The abundance counts of biofacies, as well as grain-size data and morphometric measurements of rhodoliths are available in CSV format at <https://doi.org/10.26022/IEDA/331481>³⁶ and in Excel format at <https://doi.org/10.26022/IEDA/331482>³⁷.

Technical Validation

In order to avoid magnetic interference during magnetometric acquisition (i.e., vessel interference), a distance greater than three times the ship length was established between the towed fish and the vessel. For multichannel seismic data, quality control procedures were implemented during the acquisition. The seismic streamer was towed alongside the vessel to ensure attenuation of acoustic noise generated by the vessel. Weights were added to the streamer within a specific geometry to maintain streamer depth stable throughout the acquisition, which enhances the seismic signal in the far offsets and prevents the occurrence of burst noise. The geometry of acquisition (Table 1) was tested through the modeling and comparison of the direct wave arrival in the data, during acquisition. Bin sizes were then determined to optimize the fold number in the stacked section. Further processing procedures (i.e., pre-stack migration, noise modeling) may be performed to further improve data results, depending on the investigation goals. Even so, technical limitations of using a short streamer result in a difficulty of properly imaging surfaces/areas with a high gradient, particularly along the continental slope and seamounts, where the seismic traces are often distorted and do not represent the regional stratigraphy.

Bathymetric and SBP surveys were conducted by the Brazilian Navy, which follows the bathymetric technical standards of the NORMAM 501³⁸ and IHO S-44³⁹. A multibeam patch test was conducted prior to the scientific expedition, where pitch, roll, and heave corrections were applied. Since the bathymetric survey covered deep regions, tide correction was deemed unnecessary as tide variations represent less than 1% of the minimum seafloor depth observed. The vertical extrapolation of sound velocity profiles for depths below 1800 m is a major cause of depth uncertainty in the deep part of the survey. Although sound velocity values below the thermocline

Sediment Sample	Rhodolith Specimen	Large Axis (mm)	Intermediary Axis (mm)	Short Axis (mm)
V8	1	71.16	50.49	31.91
V8	2	42.79	39.72	10.4
V8	3	44.32	34.52	29.03
V8	4	51.11	38.92	42.65
V8	5	88.91	65.12	18.43
V8	6	51.45	34.08	13.15
V8	7	55.87	37.18	18.78
V8	8	50.78	24.68	15.73
V8	9	63.09	55.78	21.77
V8	10	37.5	25.22	18.52
V8	11	50.91	42.51	10.31
V8	12	4.89	44.7	25.91
V8	13	49.81	34.7	12.06
V8	14	56.03	31.34	16.77
V8	15	48.61	35.13	8.52
V8	16	45.4	27.12	17.85
V8	17	37.24	29.35	20.65
V8	18	46.35	33.12	22.71
V8	19	37.26	29	24.35
V8	20	38.43	27.15	19
V8	21	38.47	28.49	19.63
V8	22	36.87	29.04	24.74
V8	23	34.23	31.66	17.06
V8	24	41.61	24.65	16.72
V8	25	32.89	19.27	18.98
V8	26	34.24	17.72	6.34
V8	27	30.3	20.96	19.47
V8	28	28.22	16.54	15.85
V8	29	30.76	24.82	15.02
V8	30	30.7	17.19	14.71
V8	31	30.27	16.51	12.74
V8	32	21.55	15	19.18
V8	33	32.8	20.11	11.8
V8	34	32.41	19.96	11.19
V8	35	32.07	23.33	10.3
V8	36	39.47	13.14	19.18
V8	37	24.03	22.47	12.15
V8	38	28.57	13.93	6.7
V8	39	34.37	13.59	7.64
V8	40	23.89	23.59	14.31

Table 4. Morphometric measurements for Rhodolith samples V8.

(>1000 m depths) tend to vary similarly across ocean regions, for each 1 m/s of error between calculated and real sound velocities, we can expect a bathymetric uncertainty of ~1 m at 2000 m depth and at ~3 m at 5000 m depths. For sediment analysis, sedimentological standards of Folk^{23,24} were followed. The initial and final masses were measured and when those values had a >10% difference, the analysis was repeated.

Code availability

No custom code was used in this dataset.

Received: 29 January 2024; Accepted: 19 September 2024;

Published online: 27 September 2024

References

1. Napolitano, D. C., Da Silveira, I. C. A., Tandon, A. & Calil, P. H. R. Submesoscale Phenomena Due to the Brazil Current Crossing of the Vitória-Trindade Ridge. *JGR Oceans* **126**, e2020JC016731 (2021).
2. Mohriak, W. Genesis and evolution of the South Atlantic volcanic islands offshore Brazil. *Geo-Mar Lett* **40**, 1–33 (2020).
3. Skolotnev, S. G., Bylinskaya, M. E., Golovina, L. A. & Ipat'eva, I. S. First data on the age of rocks from the central part of the Vitoria-Trindade Ridge (Brazil Basin, South Atlantic). *Dokl. Earth Sc.* **437**, 316–322 (2011).

4. Skolotnev, S. G. & Peive, A. A. Composition, structure, origin, and evolution of off-axis linear volcanic structures of the Brazil Basin, South Atlantic. *Geotecton.* **51**, 53–73 (2017).
5. Maia, T. M. *et al.* First petrologic data for Vitória Seamount, Vitória-Trindade Ridge, South Atlantic: a contribution to the Trindade mantle plume evolution. *Journal of South American Earth Sciences* **109**, 103304 (2021).
6. Napolitano, D. C., Rocha, C. B., Da Silva, I. C. A., Simoes-Sousa, I. T. & Flierl, G. R. Can the Intermediate Western Boundary Current recirculation trigger the Vitória Eddy formation? *Ocean Dynamics* **71**, 281–292 (2021).
7. *Brazilian Deep-Sea Biodiversity*. <https://doi.org/10.1007/978-3-030-53222-2> (Springer International Publishing, 2020).
8. *Abyssal Channels in the Atlantic Ocean: Water Structure and Flows*. (Springer, Dordrecht; New York, 2010).
9. Fainstein, R. & Summerhayes, C. P. Structure and origin of marginal banks off Eastern Brazil. *Marine Geology* **46**, 199–215 (1982).
10. Meirelles, P. M. *et al.* Baseline Assessment of Mesophotic Reefs of the Vitória-Trindade Seamount Chain Based on Water Quality, Microbial Diversity, Benthic Cover and Fish Biomass Data. *PLoS ONE* **10**, e0130084 (2015).
11. Lima, A. F., Faugeres, J.-C. & Mahiques, M. The Oligocene–Neogene deep-sea Columbia Channel system in the South Brazilian Basin: Seismic stratigraphy and environmental changes. *Marine Geology* **266**, 18–41 (2009).
12. Massé, L., Faugères, J. C. & Hrovatin, V. The interplay between turbidity and contour current processes on the Columbia Channel fan drift, Southern Brazil Basin. *Sedimentary Geology* **115**, 111–132 (1998).
13. Schlitzer, R. Electronic atlas of WOCE hydrographic and tracer data now available. *Eos Trans. AGU* **81**, 45–45 (2000).
14. Pinheiro, H. T., Joyeux, J.-C. & Moura, R. L. Reef oases in a seamount chain in the southwestern Atlantic. *Coral Reefs* **33**, 1113–1113 (2014).
15. Guabiroba, H. C. *et al.* Coralline Hills: high complexity reef habitats on seamount summits of the Vitória-Trindade Chain. *Coral Reefs* **41**, 1075–1086 (2022).
16. Fofonoff, N. P. & Millard, R. C. Jr J., R. C. *Algorithms for the computation of fundamental properties of seawater*. <https://repository.oceanbestpractices.org/handle/11329/10910.25607/OBP-1450> (1983).
17. Locarnini, R. A., *et al.* World Ocean Atlas 2009, Volume 1: Temperature. S. Levitus, Ed., NOAA Atlas NESDIS 68, U.S. Government Printing Office, Washington, D.C., 184 pp. (2010).
18. Antonov, J. I., *et al.* World Ocean Atlas 2009, Volume 2: Salinity. S. Levitus, Ed. NOAA Atlas NESDIS 69, U.S. Government Printing Office, Washington, D.C., 184 pp. (2010).
19. Taira, K., Yanagimoto, D. & Kitagawa, S. Deep CTD Casts in the Challenger Deep, Mariana Trench. *J Oceanogr* **61**, 447–454 (2005).
20. Sneed, E. D. & Folk, R. L. Pebbles in the Lower Colorado River, Texas a Study in Particle Morphogenesis. *The Journal of Geology* **66**, 114–150 (1958).
21. Wentworth, C. K. A scale of grade and class terms for clastic sediments. *The journal of geology* **30**, 377–392 (1922).
22. Blott, S. J. & Pye, K. GRADISTAT: a grain size distribution and statistics package for the analysis of unconsolidated sediments. *Earth Surf. Process. Landforms* **26**, 1237–1248 (2001).
23. Folk, R. L. & Ward, W. C. Brazos River bar: a study in the significance of grain size parameters. *J. Sediment. Petrol.* **27**, 3–26 (1957).
24. Folk, R. L. *Petrology of Sedimentary Rocks*. (Hemphill Pub. Co, Austin, Tex, 1980).
25. Schindelin, J. *et al.* Fiji: an open-source platform for biological-image analysis. *Nat Methods* **9**, 676–682 (2012).
26. Tagliaro, G. *et al.* Ship track navigation data for the CORE-VTRCC cruise (2021). *MGDS*. <https://doi.org/10.26022/IEDA/331475> (2024).
27. Tagliaro, G. *et al.* Raw high-resolution multi-channel seismic reflection (MCS) field data from the CORE-VTRCC cruise (2021). *MGDS*. <https://doi.org/10.26022/IEDA/331494> (2024).
28. Tagliaro, G. *et al.* Processed high-resolution multi-channel seismic reflection (MCS) data from the CORE-VTRCC cruise (2021). *MGDS*. <https://doi.org/10.26022/IEDA/331485> (2024).
29. Tagliaro, G. *et al.* Sub-bottom profiler data from the CORE-VTRCC cruise (2021). *MGDS*. <https://doi.org/10.26022/IEDA/331484> (2024).
30. Tagliaro, G. *et al.* Raw multibeam swath bathymetry data for the CORE-VTRCC cruise (2021). *MGDS*. <https://doi.org/10.26022/IEDA/331477> (2024).
31. Tagliaro, G. *et al.* Processed multibeam swath bathymetry data for the CORE-VTRCC cruise (2021). *MGDS*. <https://doi.org/10.26022/IEDA/331478> (2024).
32. Tagliaro, G. *et al.* Processed gridded bathymetry data for the CORE-VTRCC cruise (2021). *MGDS*. <https://doi.org/10.26022/IEDA/331479> (2024).
33. Tagliaro, G. *et al.* Sound velocity data for the CORE-VTRCC cruise (2021). *MGDS*. <https://doi.org/10.26022/IEDA/331480> (2024).
34. Tagliaro, G. *et al.* Magnetic field and anomaly data for the CORE-VTRCC cruise (2021). *MGDS*. <https://doi.org/10.26022/IEDA/331476> (2024).
35. Tagliaro, G. *et al.* Photographs of Vitoria Trindade Ridge Sediment Samples from the CORE-VTRCC Cruise (2021). *MGDS*. <https://doi.org/10.26022/IEDA/331483> (2024).
36. Tagliaro, G. *et al.* Sediment sample physical properties and biofacies abundance data (ASCII CSV format) for the CORE-VTRCC cruise (2021). *MGDS*. <https://doi.org/10.26022/IEDA/331481> (2024).
37. Tagliaro, G. *et al.* Sediment sample physical properties and biofacies abundance data (Excel format) for the CORE-VTRCC cruise (2021). *MGDS*. <https://doi.org/10.26022/IEDA/331482> (2024).
38. DHN – Diretoria de Hidrografia e Navegação. NORMAM-501/DHN: Normas da Autoridade Marítima para Levantamentos Hidrográficos. Marinha do Brasil, Brazil, 147 p., (2023).
39. International Hydrographic Organization. IHO Standards for Hydrographic Surveys. (2008).
40. Alberoni, A. A. L., Jeck, I. K., Silva, C. G. & Torres, L. C. The new Digital Terrain Model (DTM) of the Brazilian Continental Margin: detailed morphology and revised undersea feature names. *Geo-Mar Lett* **40**, 949–964 (2020).
41. Ryan, W. B. F. *et al.* Global Multi-Resolution Topography synthesis. *Geochem Geophys Geosyst* **10**, 2008GC002332 (2009).

Acknowledgements

We thank the Brazilian Navy and the Directorate of Hydrography and Navigation (DHN) for enabling the VTRCC cruise within the program PROAMAZONIA AZUL, and all crew members of the NHo Cruzeiro do Sul vessel for the support during the expedition. Additionally, we thank the Sedimentology Laboratory from the Geoscience Institute of the University of São Paulo where sediment analysis was performed, Alexander Nedospasov and GEOGALS consulting for the support with multichannel seismic processing, and two anonymous reviewers that helped improving the manuscript. This research was funded by FAPESP thematic project 2016/24946-9 and post-doctoral grant 2020/08847-6. The dataset is freely available at the Marine Geoscience Data System at <https://www.marine-geo.org/tools/search/entry.php?id=CORE-VTRCC#datasets>.

Author contributions

According to the CRediT (Contribution Roles Taxonomy) system: Gabriel Tagliaro contributed to conceptualization, data curation, investigation, methodology, project administration, resources, supervision, validation, visualization, writing original draft preparation and writing review & editing; Mateus A.C. Gama contributed to conceptualization, data curation, investigation, validation, visualization, writing original draft preparation and writing review & editing; Adolfo N. Britzke and Pedro Bauli contributed to data curation, investigation, methodology, validation, visualization and writing original draft preparation; Vinicius H.A. Louro contributed to, investigation, supervision, validation and writing original draft preparation; Gabriela C. Patines and Gabrielle D. Bonifatto, contributed to investigation and validation; Ana C.B. Vieira, Beatriz B.S. Silva, Geandré C. Boni, Luan K. Pantoja, Paula P. Sergipe, Raylla S. Silva, Sarah A. Dos Santos, Tainá N. Caram and Tainá L.F. Pereira contributed to investigation; Luigi Jovane contributed to funding acquisition, project administration, resources and supervision.

Competing interests

The authors declare no competing interests.

Additional information

Correspondence and requests for materials should be addressed to G.T.

Reprints and permissions information is available at www.nature.com/reprints.

Publisher's note Springer Nature remains neutral with regard to jurisdictional claims in published maps and institutional affiliations.



Open Access This article is licensed under a Creative Commons Attribution-NonCommercial-NoDerivatives 4.0 International License, which permits any non-commercial use, sharing, distribution and reproduction in any medium or format, as long as you give appropriate credit to the original author(s) and the source, provide a link to the Creative Commons licence, and indicate if you modified the licensed material. You do not have permission under this licence to share adapted material derived from this article or parts of it. The images or other third party material in this article are included in the article's Creative Commons licence, unless indicated otherwise in a credit line to the material. If material is not included in the article's Creative Commons licence and your intended use is not permitted by statutory regulation or exceeds the permitted use, you will need to obtain permission directly from the copyright holder. To view a copy of this licence, visit <http://creativecommons.org/licenses/by-nc-nd/4.0/>.

© The Author(s) 2024